THE JOURNAL OF PHYSICAL CHEMISTRY C

Article

Reactivity of Monolayer Protected Silver Clusters Towards Excess Ligand: A Calorimetric Study

Ananya Baksi, Megalamane S. Bootharaju, Pratap K. Chhotaray, Papri Chakraborty, Biswajit Mondal, Shridevi Bhat, Ramesh L. Gardas, and Thalappil Pradeep

J. Phys. Chem. C, **Just Accepted Manuscript** • DOI: 10.1021/acs.jpcc.7b07557 • Publication Date (Web): 31 Oct 2017

Reactivity of Monolayer Protected Silver Clusters Towards Excess Ligand: A Calorimetric Study

Ananya Baksi,[1] M. S. Bootharaju,[1] Pratap K. Chhotaray,[2] Papri Chakraborty,[1] Biswajit Mondal,[1] Shridevi Bhat,[1] Ramesh Gardas[2] and Thalappil Pradeep[1]*

[1]DST Unit of Nanoscience and Thematic Unit of Excellence, Department of Chemistry, Indian Institute of Technology Madras, Chennai – 600036, India.

[2]Department of Chemistry, Institute of Technology Madras, Chennai – 600036, India.

*Corresponding author, E-mail: pradeep@iitm.ac.in

ABSTRACT: Reactivity of monolayer protected atomically precise clusters of noble metals is of significant research interest. Till date very few experimental data are available on the reaction thermodynamics of such clusters. Here we report a calorimetric study of the reaction of glutathione (GSH) protected silver clusters in presence of excess ligand, GSH using isothermal titration calorimetry (ITC). We have studied $Ag_{11}(SG)_7$ and $Ag_{32}(SG)_{19}$ clusters and compared their reactivity with GSH protected silver nanoparticles (AgNPs) and silver ions. Clusters show intermediate reactivity towards excess ligand compared to nanoparticles and silver ions. Several control experiments were performed to understand the degradation mechanism of these silver clusters and nanoparticles. Effect of dissolved oxygen in the degradation process was studied in detail and found that it did not have a significant role, although alternate pathways of degradation with the involvement of oxygen cannot be ruled out. Direct confirmation of the fact that functionalized metal clusters fall in-between NPs and atomic systems in their stability is obtained experimentally for the first time. Several other thermophysical parameters of these clusters were also determined including, density, speed of sound, isentropic compressibility and coefficient of thermal expansion.

1. INTRODUCTION

Monolayer protected atomically precise clusters of noble metals are an emerging class of materials composed of well-defined metal cores and ligand shells.[1-2] Starting from phosphine ligand protection[3-5] in the early period of this work, thiol ligands are used most extensively these days. While the use of water-soluble ligands is limited,[6-10] organic-soluble thiols are commonly used for the synthesis of clusters.[11-17] Although single crystal structure is the most preferred way to understand the atomic framework of these materials, only a few silver clusters have been crystallized so far.[17-18] Most of the cluster compositions have been deduced from their optoelectronic properties and mass spectral signatures, especially in the case of silver.[6-8, 10-16, 19-31] Organic-soluble clusters are more stable than their water soluble analogues due to the inherent tendency of degradation of such species in aqueous media. Glutathione, a tri-peptide (GSH), mercaptosuccinic acid (MSA) and mercaptobenzoic acid (MBA) are the commonly used water-soluble ligands for silver cluster synthesis.[8-10, 14, 28] Among the water-soluble ligands, GSH has been used extensively for synthesizing gold and silver clusters in aqueous medium. High fluorescence quantum yield, aggregation induced luminescence enhancement, bio-viability, high degree of cellular uptake, antimicrobial activities are a few topics where intense research has happened using GSH protected noble metal clusters.[9, 28, 32-36] As mentioned, these clusters undergo degradation with time if they are in solution. The rate of degradation varies depending on the ligand and metal core composition. For example, glutathione protected silver clusters are more stable than MSA protected clusters in solution. However, there have been no systematic studies of the reactivity of clusters in the context of their thermodynamic stability in solution. The first report on alloying of different nanoparticles were studied by Toshima et al., where they found highly exothermic reactions while alloying Ag/Pd/Pt/Rh nanoparticles.[37]

Isothermal titration calorimetry (ITC) is a powerful tool to find parameters of reactions in solution.[38-39] In a typical ITC experiment, analyte is titrated against the reactant at a constant temperature. A fixed amount of reactant is injected through a syringe and a constant power is applied to maintain the same conditions in the reactant and reference cells (filled with the same solvent). While mixing of two reactants, the heat released/absorbed has to be compensated by the power supply. This change is observed as a thermograph, which may be converted to heat change, and an appropriate fit will provide the desired thermodynamic parameters. In the beginning, enough reactants are available to interact and hence one may observe a sharp heat change. As time goes on, more and more analyte is consumed and the heat change will decrease until all the analyte is consumed. Once the reaction is over, some heat change will still be observed due to heat of dilution. The peaks are integrated to acquire total heat change during the reaction. From a proper fitting of the data, binding sites (N), rate constant of the reaction (k), enthalpy change (ΔH) and entropy change (ΔS) can be calculated, using the change in Gibbs free energy (ΔG).

In the case of monolayer-protected clusters, stability depends on many factors. When there is excess ligand, it interacts with existing clusters and finally degrades to smaller chain thiolates. In a standard synthesis of thiolate protected

clusters, metal thiolates are reduced to clusters using a reducing agent in solution.[28] Thus the reverse reaction, i.e., clusters decomposing to thiolates can be used to find their thermodynamic stability.[40] This is also the case of nanoparticles protected with thiolates. In view of this, we have designed a condition to study the thermodynamic parameters of the reaction of glutathione protected silver clusters and excess glutathione, using ITC as the method. We used two different clusters, namely, $Ag_{32}(SG)_{19}$[9] and $Ag_{11}(SG)_7$[6] and the heat change was compared with Ag NPs protected with GSH. Among the various available clusters, we have chosen these two as they were characterized previously, stable in water and react with glutathione in the experimental conditions and the reaction goes to completion.

2. EXPERIMENTAL

Materials: Silver nitrate ($AgNO_3$, 99%), glutathione reduced (GSH, 97%, Aldrich), sodium borohydride ($NaBH_4$, 99.99%, Aldrich), ethanol (HPLC grade, 99.9%, Aldrich) and methanol (HPLC grade) were used as received and all the chemicals were used without further purification. MilliQ water was used throughout the experiments.

Instrumentation: Isothermal calorimetric studies were conducted in a GE Healthcare Microcal iTC200 instrument. The optimized parameters were as follows: Cell Temperature: 30-50°C; Reference Power: 8 µcal/sec**;** Initial Delay: 60 sec; Stirring speed: 500 RPM; Volume of sample in Cell (cluster, nanoparticles etc.): 200 µL and Volume of sample in syringe (GSH): 40µL.The data were fitted using Origin software. The instrument is calibrated using ethylenediaminetetraaceticacid (EDTA) and $CaCl_2$.

ESI MS analyses were carried out using a Waters Synapt HDMS instrument. Spectra were collected in the negative mode for a mass range of m/z 100-2000 and data were averaged for 300 scans. All the spectra were collected at a source voltage of 500 V. Source temperature and desolvation temperature were set at 120 and 200°C, respectively. Flow rate was set at 5 µL/min. Masslynx 4.1 software was used for analyzing the data.

For UV-vis absorption spectra, a Perkin Elmer Lambda 25 instrument was used and the spectra were collected in the range of 200-1100 nm with a band pass of 1 nm. X-ray photoelectron spectroscopy (XPS) measurements were done using an Omicron ESCA Probe spectrometer with polychromatic Mg K_α X-rays ($h\nu$ = 1253.6 eV) and the data were analyzed by CasaXPS software.

Density and speed of sound were measured using an Anton Paar (DSA 5000M) instrument. It can measure the density from 0 to 3 $g.cm^{-3}$ and speed of sound from 1000 to 2000 $m.s^{-1}$ with accuracies of 1×10^{-6} $g.cm^{-3}$ and 0.1 $m.s^{-1}$, respectively. The instrument enables us to measure both the properties simultaneously, where the temperature was controlled by built in Peltier thermostat with a temperature accuracy of 0.001°C. The instrument was calibrated with dry air and Millipore water at regular intervals of time.

Synthesis of $Ag_{11}(SG)_7$: $Ag_{11}(SG)_7$ was synthesized following a previously reported method.[6] Briefly, 650 mmol of GSH was added to 50 mL of MeOH under ice cold conditions and stirred for 10 minutes. About 130 mmol of $AgNO_3$, dissolved in 0.5 mL of Millipore water was mixed with the GSH solution and the mixture was stirred for 15 minutes to form silver thiolates. About 7 mL (1.4 mol) of ice cold sodium borohydride was added to the mixture drop-wise. The solution was stirred for another 15 minutes for complete reduction of Ag-thiolates to clusters. The as-formed clusters were not completely soluble in methanol and they started precipitating. Excess MeOH was added for complete precipitation. The sample was centrifuged at 7000 rpm and washed repeatedly with methanol to remove the excess ligand and thiolates. The precipitate was dried using rotavapor to obtain a dry powder.

Synthesis of $Ag_{32}(SG)_{19}$: $Ag_{32}(SG)_{19}$ was synthesized following the solid state synthesis method reported previously.[9] In a typical synthesis, 200 mg of glutathione (GSH) was mixed and ground with 23 mg of $AgNO_3$ using a mortar and pestle. Thus formed AgSG thiolates were reduced by 50 mg of $NaBH_4$. Successful cluster formation was confirmed by the color change to dark brown. The sample was dissolved in deionized water and excess MeOH was added to precipitate the cluster. The precipitate was centrifuged at 8000 rpm and washed repeatedly with MeOH. The reddish brown sample was then freeze dried to get a dry powder.

Synthesis of AgNPs@SG: Ag NPs were synthesized in solution by mixing 8.5 mg of $AgNO_3$ in 100 mL of 1 mM aqueous GSH. The color changed from colorless to pale yellow. The AgSG thiolates in solution were reduced by 1 mM 7 mL $NaBH_4$. Once the solution changed to yellow, 15 mg GSH was added and the mixture was incubated for 4 h till a dark yellow solution was achieved.

Measurement of pH: In order to compare the true change in pH during degradation of the cluster, the following experiment was performed. To 1 mM of $Ag_{32}(SG)_{19}$, fixed volumes of 10 mM GSH was added and the pH change was measured after 10 min. Data corresponding to 5 such additions are presented in supporting information. As free GSH, upon dilution, can also result in a pH change, this effect was subtracted by conducting a separate experiment. In this, the pH change due to dilution of GSH was measured after each aliquot as above (5 in all).

3. RESULTS AND DISCUSSION

3.1. Reaction of $Ag_{32}(SG)_{19}$ *vs.* GSH

$Ag_{32}(SG)_{19}$ and $Ag_{11}(SG)_7$ were prepared following the previously reported methods.[6, 9] In view of their reported properties, characterization of clusters is not discussed here. About 1 mM purified cluster solution was used for the reaction and the ligand concentration was varied accordingly to get a proper saturation curve in ITC. Figure 1A shows a real time thermograph of $Ag_{32}(SG)_{19}$ *vs.* GSH titration (top) and corresponding heat change is shown in the bottom panel. The data were fitted using a one site model and the corresponding thermodynamic properties are listed in Table 1. Different fitting models were tried but the best fit was achieved using the one site model and hence all the data presented here were fitted using this model.

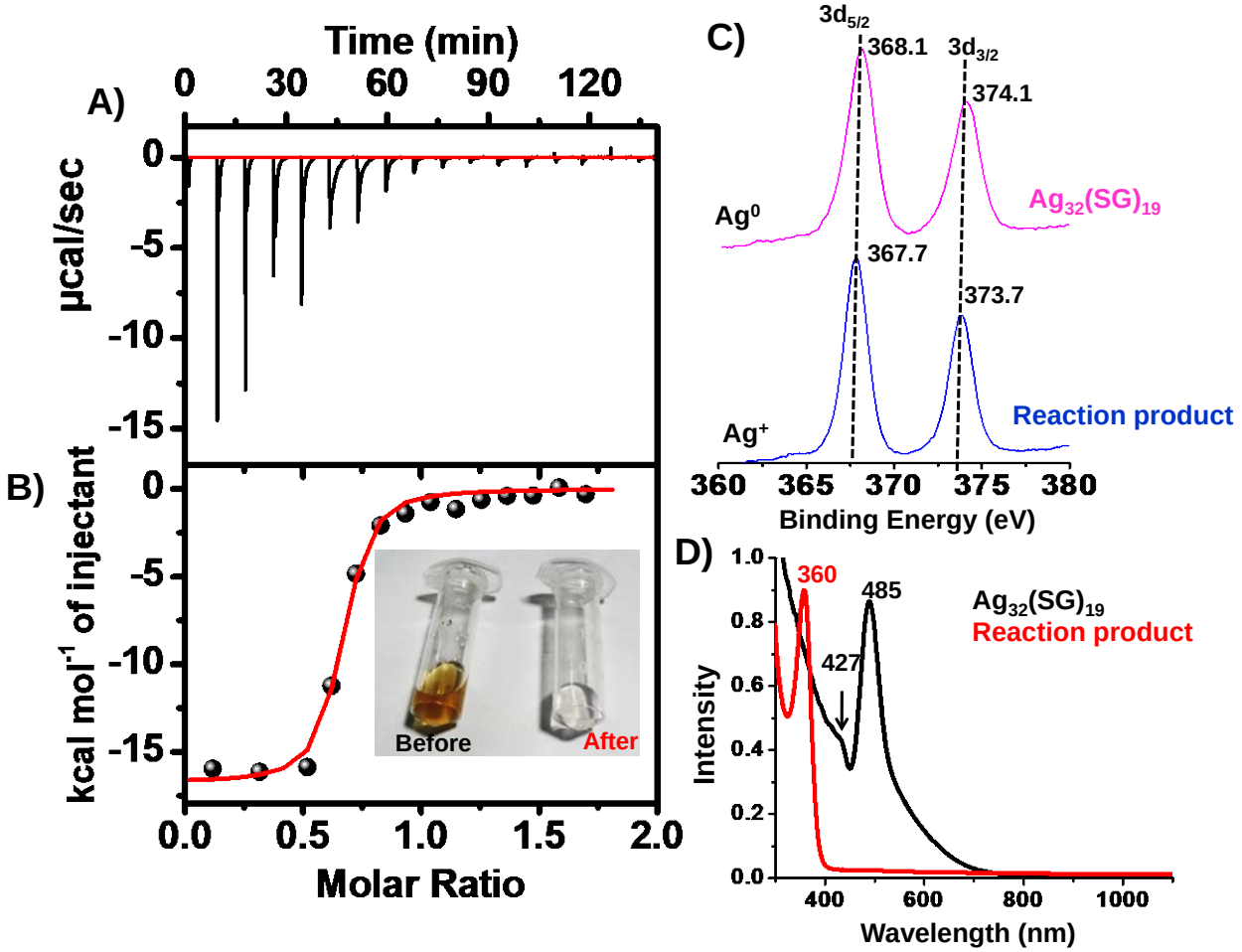

Figure 1: A) Real time isothermal titration calorimetric data of $Ag_{32}(SG)_{19}$(1 mM) vs. GSH (10 mM) (top) and B) respective heat change data (bottom). The data were fitted with a one site model and the thermodynamic parameters obtained are listed in Table 1. Photographs of the cluster before and after reaction are shown as inset of B. During titration, colored $Ag_{32}(SG)_{19}$ clusters react with GSH and form colorless thiolates where silver is in Ag^+ state as revealed from XPS, shown in C). UV-vis absorption spectra D) of $Ag_{32}(SG)_{19}$ before and after titration with GSH.

In the one site model, it is assumed that the cluster has one type of binding site; which may be multiple number of identical sites, in terms of reactivity. We have performed several concentration-dependent studies to get the exact ratios of cluster and glutathione. At lower concentrations of GSH (5 mM) (see Figure S1), the binding constant was lower (3.5×10^4 M^{-1}) and it took longer time to reach the end point. At a higher concentration of GSH (10 mM), the binding constant was larger (1.88×10^5 M^{-1} which is 5.3 times faster than the reaction with 5 mM GSH). At intermediate concentration (7.5 mM) (see Figure S2), we achieved a moderate binding constant (8.5×10^4 M^{-1} which is 2.4 times higher than the reaction with 5 mM GSH and 2.2 times lower than the reaction with 10 mM GSH) as well as saturation. The data clearly suggest that the degradation of clusters to thiolates is directly proportional to the excess ligand in the medium.

For better understanding of the parameter K, the reaction happening within the microcalorimeter should be understood. Microcalorimeters are used typically to understand the interaction of biomolecules such as proteins, DNA, etc. with various ligands and the experimental parameters are also termed accordingly. Models are written generally in this context. In a typical macromolecule-ligand reaction, there is a non-covalent interaction to form a complex. There are three species in equilibrium in the solution that are receptor, free incoming ligand and the complex formed. The reaction is always considered to be first order. Fundamental understanding of the interaction can be achieved from equilibrium constant (binding constant) K for a binding process with binding stoichiometry N (how many molecules of the incoming ligand can bind to the receptor at saturation) as given below:

Cluster + Glutathione $\rightleftharpoons$ Thiolate

$$K_{eq} = \left\{ \frac{[\text{Thiolate}]}{[\text{Cluster}]\,[\text{Glutathione}]} \right\}_{eq}$$

$$\Delta G^\circ = -RT\ln K_{eq}$$

$$\Delta G = \Delta G^{\circ} + RT \ln \left\{ \frac{[\text{Thiolate}]}{[\text{Cluster}]\,[\text{Glutathione}]} \right\}_{\text{actual}}$$

$$\Delta G = \Delta H - T\Delta S$$

Where, K_{eq} or K is the equilibrium constant, [X] is molar equilibrium or actual concentration of species X, ΔG° is standard Gibbs free energy change, R is universal gas constant, T is temperature in Kelvin, ΔG is actual free energy change and ΔS is the entropy change for complex formation.[41-42] The reaction studied may also be considered as first order or pseudo-first order, when pH is not changing significantly and when one of the reagents is in excess.

In all cases, the reactions are exothermic in nature. As two species are reacting to give one type of product, the entropy change is negative. Overall free energy is negative (-7.28×10^{3}cal/mol) mainly due to highly negative enthalpy change (-1.67×10^{4}cal/mol). So the reaction is thermodynamically favorable and enthalpy driven. Consolidated data are listed in Table 1.

Table 1: Thermodynamic parameters of $Ag_{32}(SG)_{19}$ vs. GSH at different reaction conditions.

S/N	Cluster (mM)	GSH (mM)	N (Sites)	$k\times10^{3}$ (M^{-1})	$\Delta H\times10^{4}$ (cal/mol)	ΔS (cal/ deg.mol)	T (K)	$\Delta G\times10^{3}$ (cal/mol)
1	1	05.0	0.50	035.0	-2.56	-53.40	303	-9.42
2	1	10.0	0.60	188.0	-1.67	-31.10	303	-7.28
3	1	07.5	0.50	085.2	-2.26	-53.90	303	-6.27
4	1	07.5	0.60	011.4	-2.48	-60.40	313	-5.80
5	1	07.5	0.60	009.9	-2.98	-74.20	323	-5.83

$Ag_{32}(SG)_{19}$ was well characterized by mass spectrometry in the previous work by Rao *et al.*[9] After the reaction, the product was analyzed by ESI MS which showed peaks at m/z 414, 1134, 935, and 1548 due to $AgSG^{-}$, $Ag_2(SG)_3^{-}$, $Ag_3(SG)_2^{-}$, and $Ag_3(SG)_4^{-}$, respectively[6, 9] (see Figure 2). All of these thiolates are formed when Ag^{+} reacts with GSH. From the experimental ITC data, binding sites are always less than one which can be justified in terms of the conversion of a cluster to linear thiolates, $(AgSG)_n$. In $Ag_{32}SG_{19}$, the SG:Ag ratio is 0.59, which becomes 1 in a linear $(AgSG)_n$ thiolate. Thus the increase in binding sites is only 0.41. The value measured is 0.6, difference observed appears to be due to the various linear thiolates formed, which have larger SG:Ag ratios. Reaction between 1 mM $Ag_{32}(SG)_{19}$ and 10 mM GSH is shown in Figure 1A. Photographs of the cluster before and after reaction are shown in the inset of B). As all the clusters have degraded, the solution became colorless (Ag thiolates are colorless) which is clearly visible in the photographs.

This was again proven from an XPS study where oxidation state of silver has changed from 0 to +1 confirming the degradation of the cluster in presence of excess glutathione. Note that in the case of Ag(I), the binding energy (BE) is lower than in Ag(0) by 0.5 eV.[43] The cluster to begin with is close to Ag(0) and after the reaction the BE is lowered. The data were further verified using UV-vis absorption spectroscopy. $Ag_{32}(SG)_{19}$ cluster has characteristic peaks at 485and 427 nm which are completely absent after reaction with GSH and a sharp peak appeared at 360 nm due to thiolate formation, which was independently tested.[9] Previous reports by Shen *et al.*, and Bellina *et al.*, on Ag-thiolates suggest the absorption maximum to be around 260-280 nm.[44-45] When GSH and Ag^{+} react separately, the thiolates formed show absorption at ~280 nm[44-45] along with another peak at 360 nm. While the peak at 280 nm was attributed to smaller thiolates, the latter at 360 nm was attributed to polymeric $(AgSG)_{\infty}$.[45] In the present study, similar absorption feature was observed for the products obtained from the reaction of clusters or nanoparticles (see later) with excess GSH. In this process, GSH can react with each other and dimeric and polymeric GSSG may form. While smaller thiolates could be detected by ESI MS, the polymeric thiolates were too heavy and could not be detected.

The reaction was conducted at three different temperatures (see Figure S3 and S4). The data are listed in Table 1.

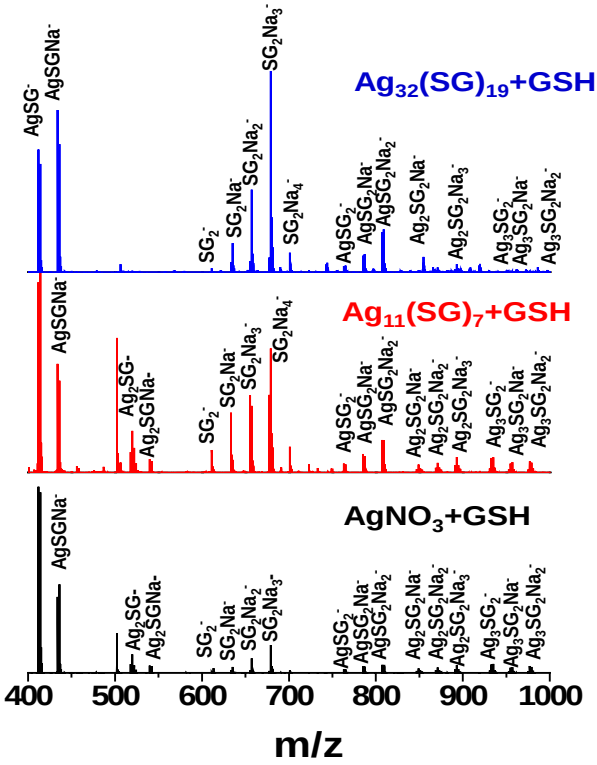

Figure 2. A) ESI MS of reaction product of $AgNO_3$, $Ag_{11}(SG)_7$ and $Ag_{32}(SG)_{19}$ with excess GSH showing formation of similar thiolates.

3.2. Reaction of $Ag_{11}(SG)_7$ *vs.* GSH

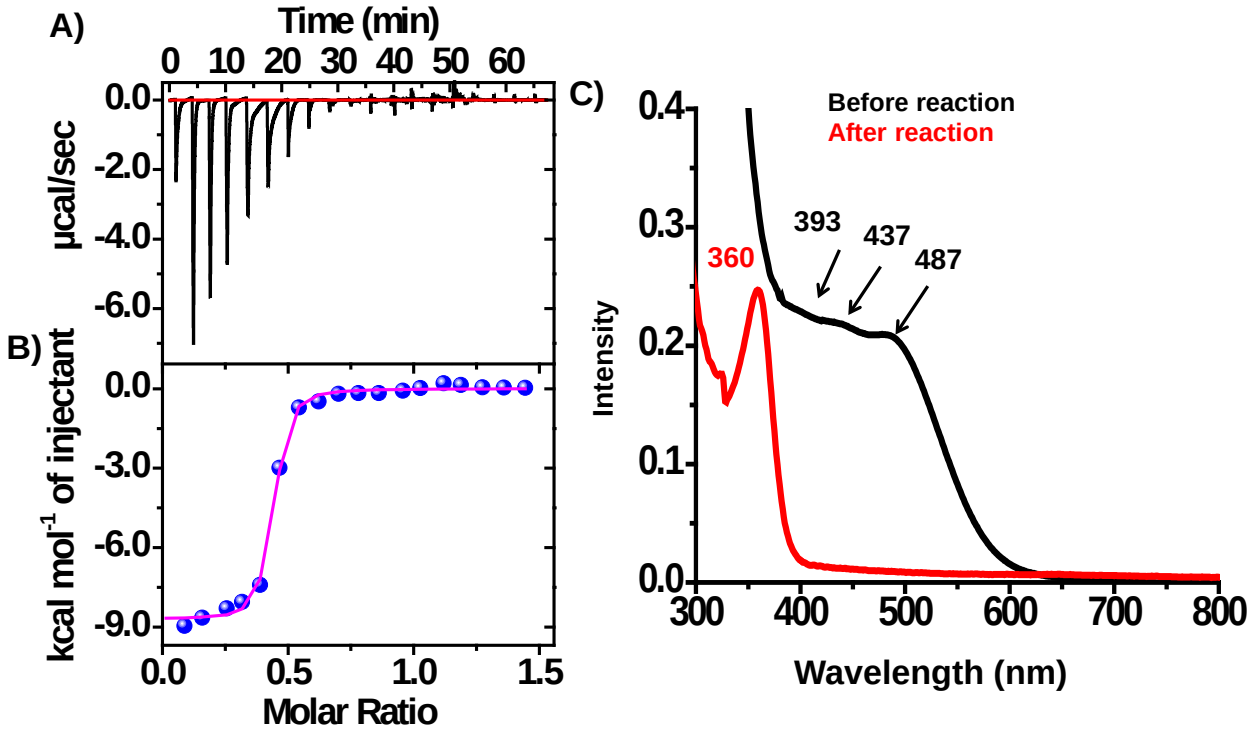

Figure 3. A) Real time isothermal titration calorimetric data of $Ag_{11}(SG)_7$ vs. GSH (top) and B) respective heat change data (bottom). C) UV-vis absorption features of $Ag_{11}(SG)_7$ before and after reaction with excess GSH.

To validate our method, we have used another glutathione protected Ag cluster, $Ag_{11}(SG)_7$ for a similar degradation study. In this case, degradation of the cluster in presence of excess GSH was faster than for $Ag_{32}(SG)_{19}$ under similar reaction conditions indicating less stability of the $Ag_{11}(SG)_7$ cluster in the mentioned experimental condition. When 1 mM $Ag_{11}(SG)_7$ was reacted with 7.5 mM of GSH, the reaction was almost complete within 5 injections and the binding constant was 5.15×10^5 M^{-1}, 6 times higher than the binding constant of $Ag_{32}(SG)_{19}$ under similar conditions (Figure 3). The reaction is strongly enthalpy driven which dominates the total free energy change and is more negative than $Ag_{32}(SG)_{19}$ (see Table 1 and 2 for comparison). Entropy obtained during degradation of $Ag_{32}(SG)_{19}$ was more negative than $Ag_{11}(SG)_7$ [ΔS = -2.59 cal/deg.mol for $Ag_{11}(SG)_7$ and ΔS = -31.1 cal/deg.mol for $Ag_{32}(SG)_{19}$].

Note that AgSG is not the only thiolate that is formed during the degradation process, some other thiolates such as $Ag_2(SG)_3$, $Ag_4(SG)_4$ were also formed (Figure 2). Also note that, these are not written as a redox reaction and may be used purely for understanding the mechanism. There might be many other pathways and steps which are involved in the degradation process. In the present study, only the lowering of pH through proton release is observed (see later).$Ag_{11}(SG)_7$ has three characteristic absorption features at 487, 437 and 393 nm which disappeared after the reaction with the appearance of a new peak at 360 nm due to thiolates. In $Ag_{11}(SG)_7$cluster, SG:Ag ratio is 0.63. After thiolate formation, it is expected to create a binding site increase of 0.37. The experimental binding site was found to be 0.41 which is due to different types of thiolates as discussed in case $Ag_{32}(SG)_{19}$. A temperature dependent study (Figure S6) suggests that the products formed are comparable and the total free energy change in all the cases is nearly the same. The data are listed in Table 2.

Table 2: Thermodynamic parameters of $Ag_{11}(SG)_7$ vs. GSH at different reaction conditions.

S/N	Cluster (mM)	GSH (mM)	N (Sites)	k×10^5 (M^{-1})	ΔH (cal/mol)	ΔS (cal/ deg.mol)	T (K)	ΔG (cal/mol)
1	1	7.5	0.41	5.51	-8706	-2.59	303	-7921
2	1	7.5	0.50	2.05	-13510	-17.5	323	-7857

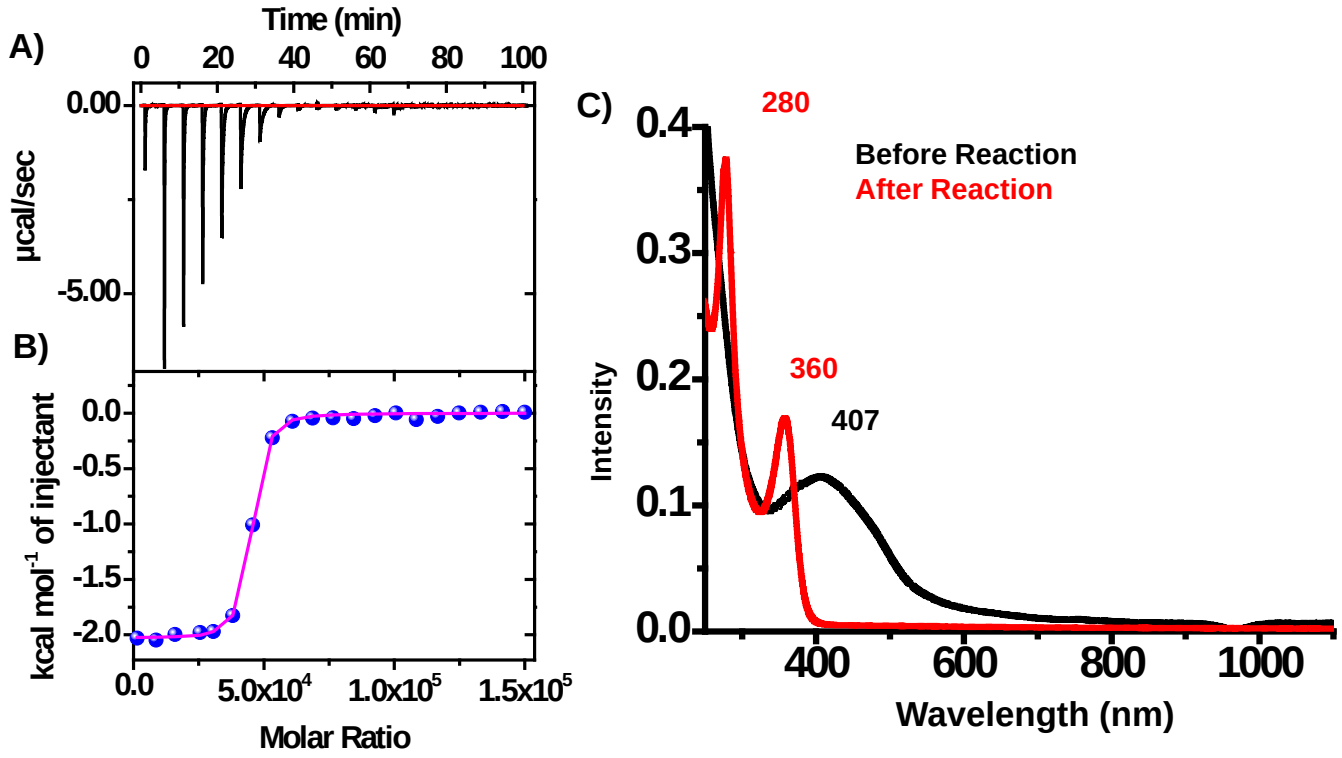

Figure 4. A) Real time isothermal titration calorimetric data of AgNP vs. GSH (top) and B) respective heat change data (bottom). C) UV-vis absorption feature of AgNPs before and after reaction with excess GSH.

3.3. **Reaction of AgNP@SG *vs.* GSH**

We have further extended our study to GSH capped AgNPs. We have synthesized AgNPs protected with GSH of ~ 20 nm diameter and carried out the ITC study (Figure 4). Detailed characterization of the nanoparticles is shown in Figure S6 and S7. When 10 mM GSH was allowed to react with 3.6×10^{-8} mM of AgNP, we found a large enthalpy change (-3.43×10^{9} cal/mol). The reaction is dominated by enthalpy.

The binding constant was found to be very high (10^5 times more than the clusters, note that here all the rates are in M^{-1}. Also note that, all the rate constants are presented as per mol of reactant). High number of binding sites indicate involvement of core Ag atoms in the reaction to form thiolates which is reflected in the UV-vis absorption spectra. Typically, AgNPs show a surface plasmon band centered at 407 nm which was absent after the degradation, and two new peaks at 280 nm and 360 nm (similar to $Ag_{32}(SG)_{19}$ and $Ag_{11}(SG)_7$ cases). At lower GSH concentrations (7.5 mM), there is a shoulder peak at 407 nm indicating the incomplete degradation of the AgNPs to thiolates, indicating incomplete reaction (Figure S8). The thermodynamic parameters are listed in Table 3.

Table 3: Thermodynamic parameters of AgNP@SG vs. GSH reaction.

S/N	AgNP×10^{-8} (mM)	GSH (mM)	N×10^4 (Sites)	k×10^{10}(M^{-1})	ΔH×10^9 (cal/mol)	ΔS×10^6 (cal/deg.mol)	T (K)	ΔG×10^6 (cal/mol)
1	3.6	07.5	2.94	1.18	-1.51	-5.06	298	-1.46
2	3.6	10.0	4.18	2.28	-2.79	-9.36	298	-1.50

3.4. **Reaction of $AgNO_3$ *vs.* GSH**

Finally, we compared these reactions with Ag^+ *vs.* GSH reaction where we used 1 mM $AgNO_3$ and titrated against 10 mM GSH. Here, we observed nearly 1:1 binding of GSH towards Ag^+ (Figure 5). The thiolate formed in this reaction is also comparable with the degradation product of the two clusters studied. This observation was supported by comparing the ESI MS data of the thiolates formed by direct reaction of Ag^+ and GSH with degradation product of the clusters. In both the cases, the thiolates formed are similar in nature (Figure 2).

Looking carefully into gold/silver cluster structure, they have a core, generally composed of metals in oxidation state (0), and the shell is always made of metal thiolates (M-SR), where the metal is in +1 oxidation state (+1 for Ag/Au) and the ligand is RS^-. Thus ligand protected clusters can be represented as $M(0)_nM(I)_mSR_y$. Generally, m = y as -SR is in the thiolate (SR^-) form. However, in several cases, m and y are not the same. Besides, there can also be an overall charge of the cluster to attain a stable electronic structure and the formula becomes, $M(0)_nM(I)_mSR_y(z\pm)$. For example, $Au_{25}SR_{18}$ has 18 thiolates which makes it possible to be considered as $Au(0)_7Au_{18}(I)SR_{18}$; in this case, the cluster as a whole acquires one electron to make a closed shell structure (of 8 electrons, counting one electron each of Au_7 and one extra charge). The structure may be formally considered as $Au(0)_7Au_{18}(I)SR_{18}(-)$. Thiols have great affinity towards Au/Ag in any form and they can interact to form respective thiolates. So the reaction could be written as follows:

$$M(0)_nM(I)_mSR^-_m + nRS^-H^+ \rightarrow n+m\ M(I)\text{-}SR^- + nH^+$$

Please note that the equation is not charge balanced. Detailed mechanism is given below. The number of protons released may be different depending on the charge state of the cluster. One important aspect that can be checked to ascertain the reaction is the change in pH. We see that the pH decreased slightly during the decomposition reaction (Figure S9) when the experiment was done outside the calorimeter keeping the same final concentration of the reactant as discussed earlier.

During addition of GSH to pure water or cluster solution, pH of the solution decreases from the initial pH and hence pH change is denoted with a negative sign. Change of pH during addition of GSH to water was subtracted from pH change during addition of GSH to the cluster solution and this value was denoted as ΔpH. As pH change during GSH addition to cluster was higher than its addition to water, ΔpH value appears negative. During reaction of 10 mM GSH with 1 mM $Ag_{32}(SG)_{19}$, overall pH change was -0.73. The pH change due to dilution of 10 mM GSH was -0.60 and hence ΔpH was -0.13. Therefore, the additional lowering of pH was due to the release of protons during the degradation process. Estimated ΔpH for the degradation was -0.09 which is close to the observed value of -0.13, for $Ag_{32}(SG)_{19}$. The observed variation may arise due to other factors such as additional reaction pathways involved as discussed earlier, variation in ionization in presence of thiolates, etc. Similarly, for the reaction of 1 mM $Ag_{11}(SG)_7$ vs. 7.5 mM GSH, the estimated ΔpH was -0.12, close to the experimental value of -0.10.

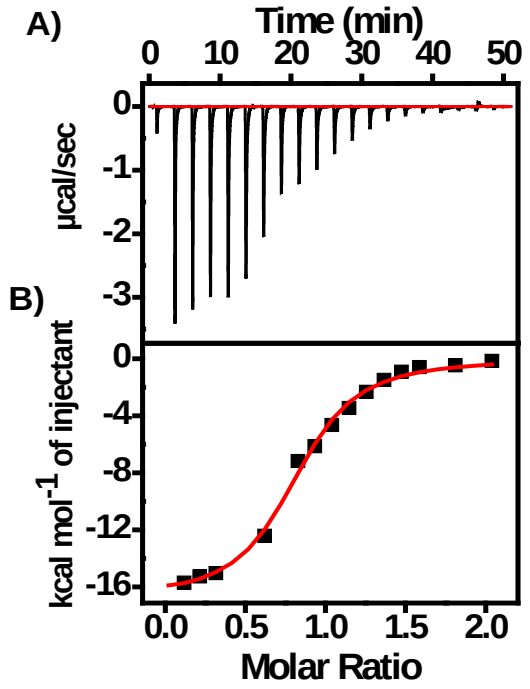

Figure 5. A)Real time isothermal titration calorimetric data of $AgNO_3$(1 mM) vs. GSH (10 mM) (top) and B) respective heat change data at 303 K (bottom).

3.5. Effect of Oxygen:

This reaction can be affected by dissolved oxygen in the medium as shown recently by Ackerson *et al.* where they have studied thiol induced etching of nanoparticles and the role of dissolved oxygen in the process.[46] As the reaction was performed solely in water, there is a high probability that dissolved oxygen may play some role. This can result in various oxygenated sulphur species. In an experimental set-up, it was not possible to maintain perfect inert atmosphere in the reaction cell while doing the experiment in a standard microcalorimeter. However, for any experiment done in a microcalorimeter, it is a general practice to purge the sample with nitrogen to avoid air bubbles, the presence of which can lead to large heat change, and the data could be misleading. Same procedure was followed here too. Therefore, the effect of dissolved oxygen is expected to be less significant here. Thermograph obtained from with and without nitrogen purging for the samples were compared and there was not much difference in the results. The comparison is shown in Supporting Information (Figure S10) and the data are listed in Table 4. From the data it is clear that dissolved oxygen is not playing role in the degradation process. It may have some role in longer time scale which is not of relevance to the present study.

Table 4: Comparison among thermodynamic parameters of 1 mM $Ag_{32}(SG)_{19}$ vs. 10 mM GSH with and without N_2 purging.

	N (Sites)	$k\times10^3$ (M^{-1})	$\Delta H\times10^4$ (cal/mol)	T (K)	ΔS (cal/deg.mol)	$\Delta G\times10^3$ (cal/mol)
With N_2 purging	0.60	188.0	-1.67	303	-31.1	-7.28
Without N_2 purging	0.63	200.0	-1.61	303	-29.1	-7.31

To understand the effect of dissolved oxygen in more detail, a systematic study was performed. Experimental conditions used during ITC measurement were reproduced in normal laboratory condition (outside the ITC instrument) where better control on parameters is possible. $Ag_{11}(SG)_7$ cluster was used for this study. The concentration of cluster and GSH obtained from ITC experiment for complete degradation of the cluster was used in this case. Briefly, about 1 mM cluster was dissolved in milliQ water and 10 mM GSH was added and UV-vis absorption spectra were monitored for the mixture. Nitrogen was purged in milliQ water for 1 h and the water was used for dissolving the cluster and GSH. All dilution was also performed with N_2 purged water for UV-vis studies. This N_2 purged water is expected to be free of any dissolved oxygen and the data obtained was used as standard for comparison. The data are compared in Figure 6. Degradation of the cluster in presence of excess GSH followed similar order in both N_2 purged and regular milliQ water which indicates there might not be any effect of the dissolved oxygen. In a similar ways O_2 was purged for an hour and the water was used as O_2 rich water. In this case, the degradation of the cluster was faster than N_2 purged water. This increased degradation rate is expected when excess oxygen is present along with excess ligand. To understand the true effect of O_2, an oxygen scavenger was used to scavenge the O_2 in O_2 rich water and the degradation study was performed in O_2 depleted water. Ascorbic acid (AA) is a well-known oxygen scavenger in aqueous system. The cluster was stable in ascorbic acid for sufficiently long time without any change (Figure S11). About 1 mM of AA was added in O_2 rich water and the degradation kinetics was comparable with N_2 purged system which signifies that there might be synergetic effect of higher concentration O_2 along

excess ligand although O_2 alone could not degrade the cluster in the absence of excess ligand.

To confirm this claim, the reaction was conducted in ITC where O_2 purged water was used as the diluent for the cluster as well as GSH. The thermodynamic parameters obtained from the experiment are listed in Table 5 (see Figure S12). The data clearly show that dissolved oxygen does not contribute to the degradation process to a large extent. However, there could be small contribution from oxygen, which cannot be evaluated by the current experimental setup.

Although we have studied the role of oxygen in detail but we note that complete removal of oxygen was not possible in normal atmospheric conditions. There could always be some oxygen, which may be involved in the degradation or to catalyze the process. From the present study it cannot be confirmed which pathway is more favorable. We believe that there could be multiple other pathways involved in this process. However, the current experiment shows a path to understand the stability and reactivity of such cluster systems and may shed light into their lower stability compared to their thiolates or nanoparticle analogues.

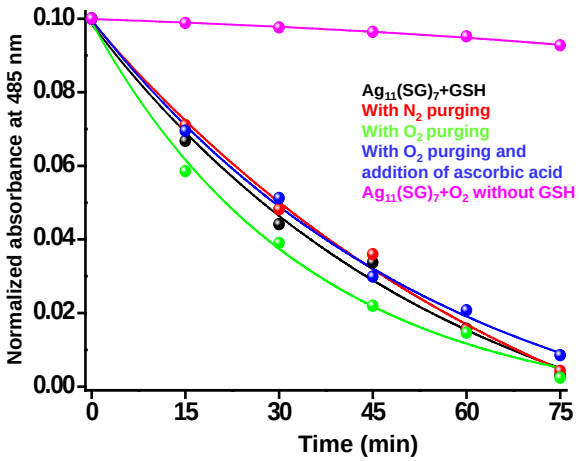

Figure 6: Degradation of $Ag_{11}(SG)_7$ cluster at various condition studied using UV-vis absorption spectroscopy. The absorbance values at 485 nm were normalized and plotted against time.

Apart from the equations stated above, the following reactions may happen during the degradation (considering involvement of O_2 in the degradation process):

$Ag_{32}(SG)_{19}$+ 13GSH→32AgSG+13H+ +13e-

$O_2(g)+4H^+ +4e^- \rightarrow H_2O$

$Ag_{32}(SG)_{19}+13/4O_2 \rightarrow 13/2H_2O(l)+32AgSG$

Considering an alternate pathway (without the involvement of oxygen):

$Ag_{32}(SG)_{19}$+ 13GSH→32AgSG+13H+ +13e-

$13/2GSSG+13H^+ +13e^- \rightarrow 13GSH$

And polymerization of AgSG

$mAgSG \rightarrow (AgSG)_\infty$

could also occur.

Table 5: Comparison among thermodynamic parameters of 1 mM $Ag_{11}(SG)_7$ vs. 7.5 mM GSH with and without O_2 purging.

S/N	Cluster (mM)	GSH (mM)	N (Sites)	k×10^5 (M^{-1})	ΔH (cal/mol)	ΔS (cal/deg.mol)	T (K)	ΔG (cal/mol)
1	1	7.5	0.41	5.51	-8706	-2.59	303	-7921
2	1	7.5	0.52	5.72	-8452	-1.91	303	-7870

3.6. Other Thermodynamic Parameters

We have studied other thermophysical properties such as density (ρ), speed of sound (u), isentropic compressibility ($\beta s = 1/\rho . u^2$) and coefficient of thermal expansion (α) for both the reactants and products (see Figure S13-S17). Same concentration (as used for ITC experiments) of reactants was used. At the experimental condition, 1.93×10^{19}, 6.4×10^{18} and 1.4×10^{19} number of Ag atoms are present in 1 mL of $Ag_{32}(SG)_{19}$, $Ag_{11}(SG)_7$ and AgNP, respectively. Considering that the contribution of total density is through the heavier Ag atoms, almost similar density is expected for all the reactants. We also have observed almost the same (experimental) density in the reaction condition. When the thiolates are formed, due to their small size, the compactness is more compared to its starting materials, which enhances the density significantly. As $Ag_{32}(SG)_{19}$ degradation leads to more number of smaller thiolates compared to $Ag_{11}(SG)_7$ and AgNP (at the concentration used for each sample), the product density is more in the case of $Ag_{32}(SG)_{19}$ + GSH. The higher values of sound velocity in the case of thiolates ($Ag_{11}(SG)_7$ + GSH, $Ag_{32}(SG)_{19}$ + GSH) also reveals that thiolates are packed more tightly as compared to corresponding clusters.$AgNO_3$and $AgNO_3$+GSH show almost equal sound velocity, probably due to similar structural arrangements. By considering the uncertainty associated with the measurements, the thermal expansion coefficients (α) of the studied systems indicate that there is an equal effect of expansion when subjected to temperature. Furthermore, the isentropic compressibility (βs) data indicate that thiolates are less compressible as compared to corresponding clusters and the values decreased from $AgNO_3$ + GSH to $Ag_{32}(SG)_{19}$ + GSH as the number of small size thiolates increased. As most of the parameters are highly dependent on concentration and not exactly on the nature of the sample, some of the data are quite similar.

4. SUMMARY AND CONCLUSIONS

In summary, we have studied thermodynamic properties of monolayer protected clusters for the first time. Reaction of excess ligand with clusters and NPs formed thiolates which were identical irrespective of the starting materials, as revealed by UV-vis absorption spectra and mass spectra. All the reactions were thermodynamically favorable and mostly enthalpy driven. We have performed detailed concentration and temperature dependent reactions for clusters and compared the data with nanoparticles. From the concentration dependent study, it was confirmed that the rate of degradation of clusters to thiolates is directly proportional to the concentration of excess ligands present in the medium, although the rate differs for different clusters as seen for $Ag_{32}(SG)_{19}$ and $Ag_{11}(SG)_7$. The rate of degradation was enhanced at higher temperature.

From the data it is clear that clusters possess intermediate stability compared to metal ions and NPs. Dissolved oxygen does not have much effect in the degradation process although slight enhancement in the rate of degradation was observed. This study would help to choose the right cluster system for different applications in solution. Although the exact mechanism of degradation is not fully understood from the current study, this is the first attempt towards understanding such a complex phenomenon using calorimetric approaches. Several other cluster systems should be tried to obtain one-to-one correlation between various factors responsible. The pH decrease observed may happen due to some other factors also which could not be understood from the present study. Further extension of this study to organic-soluble gold and silver clusters would reveal the enhanced thermodynamic stability of some clusters. The current finding of ligand induced degradation in solution will give an idea about the applicability of the specific cluster in realistic situations. Once the reaction with the same ligand which protects the cluster is understood in detail, the studies may be extended to other ligand systems.

ASSOCIATED CONTENT

Temperature and Concentration dependent ITC thermograph, UV-vis absorption spectra, density, speed of sound, isentropic compressibility, coefficient of thermal expansion vs. temperature plots are supplied as Supporting Information. “This material is available free of charge via the Internet at http://pubs.acs.org.”

AUTHOR INFORMATION

Corresponding Author

*Thalappil Pradeep, E-mail: pradeep@iitm.ac.in

Present Addresses

Ananya Baksi has moved to Karlsruhe Institute of Technology, Germany. M. S. Bootharaju has moved to King Abdullah University of Science and Technology, Saudi Arabia. Pratap K. Chhotaray has moved to Department of Chemistry, The University of Alabama, Tuscaloosa, AL 35487, USA.

Author Contributions

The manuscript was written through contributions of all authors. All authors have given approval to the final version of the manuscript.

ACKNOWLEDGMENT

A.B. and T.P. thank the Department of Science and Technology, Government of India for continuous support our of research program on nanomaterials. A.B. thanks Indian Institute of Technology Madras for fellowship.

Note

The authors declare no competing financial interest.

REFERENCES

1. Jin, R. Quantum Sized, Thiolate-Protected Gold Nanoclusters. *Nanoscale* **2010**, *2*, 343-362.
2. Mathew, A.; Pradeep, T. Noble Metal Clusters: Applications in Energy, Environment, and Biology. *Part. Part. Syst. Charact.* **2014**, *31*, 1017-1053.
3. Bellon, P.; Manassero, M.; Sansoni, M. Crystal and Molecular Structure of Triiodoheptakis[Tris(P-Fluorophenyl)Phosphine]Undecagold. *J. Chem. Soc., Dalton Trans.* **1972**, 1481-7.
4. Briant, C. E.; Theobald, B. R. C.; White, J. W.; Bell, L. K.; Mingos, D. M. P.; Welch, A. J. Synthesis and X-Ray Structural Characterization of the Centred Icosahedral Gold Cluster Compound $[Au_{13}(PMe_2Ph)_{10}Cl_2](PF_6)_3$; the Realization of a Theoretical Prediction. *J. Chem. Soc., Chem. Commun.* **1981**, *0*, 201-202.
5. Schmid, G.; Pfeil, R.; Boese, R.; Bandermann, F.; Meyer, S.; Calis, G. H. M.; van der Velden, J. W. A. $Au_{55}[P(C_6H_5)_3]_{12}Cl_6$ — Ein Goldcluster Ungewöhnlicher Größe. *Chemische Berichte* **1981**, *114*, 3634-3642.
6. Baksi, A.; Bootharaju, M. S.; Chen, X.; Hakkinen, H.; Pradeep, T. $Ag_{11}(SG)_7$: A New Cluster Identified by Mass Spectrometry and Optical Spectroscopy. *J. Phys. Chem. C* **2014**, *118*, 21722-21729.
7. Kumar, S.; Bolan, M. D.; Bigioni, T. P. Glutathione-Stabilized Magic-Number Silver Cluster Compounds. *J. Am. Chem. Soc.* **2010**, *132*, 13141-13143.
8. Udaya Bhaskara Rao, T.; Pradeep, T. Luminescent Ag_7 and Ag_8 Clusters by Interfacial Synthesis. *Angew. Chem. Int. Ed.* **2010**, *49*, 3925-3929.
9. Udayabhaskararao, T.; Bootharaju, M. S.; Pradeep, T. Thiolate-Protected Ag_{32} Clusters: Mass Spectral Studies of Composition and Insights into the Ag-Thiolate Structure from Nmr. *Nanoscale* **2013**, *5*, 9404-9411.
10. Udayabhaskararao, T.; Sun, Y.; Goswami, N.; Pal, S. K.; Balasubramanian, K.; Pradeep, T. Ag_7Au_6: A 13-Atom Alloy Quantum Cluster. *Angew. Chem., Int. Ed.* **2012**, *51*, 2155-2159.
11. Abdul Halim, L. G.; Ashraf, S.; Katsiev, K.; Kirmani, A. R.; Kothalawala, N.; Anjum, D. H.; Abbas, S.; Amassian, A.; Stellacci, F.; Dass, A.; et al. A Scalable Synthesis of Highly Stable and Water Dispersible $Ag_{44}(SR)_{30}$ Nanoclusters. *J. Mater. Chem. A* **2013**, *1*, 10148-10154.
12. Adhikari, B.; Banerjee, A. Facile Synthesis of Water-Soluble Fluorescent Silver Nanoclusters and HgII Sensing. *Chem. Mater.* **2010**, *22*, 4364-4371.
13. Bakr, O. M.; Amendola, V.; Aikens, C. M.; Wenseleers, W.; Li, R.; Dal Negro, L.; Schatz, G. C.; Stellacci, F. Silver Nanoparticles with Broad Multiband Linear Optical Absorption. *Angew. Chem. Int. Ed.* **2009**, *121*, 6035-6040.
14. Bertorelle, F.; Hamouda, R.; Rayane, D.; Broyer, M.; Antoine, R.; Dugourd, P.; Gell, L.; Kulesza, A.; Mitric, R.; Bonacic-Koutecky, V. Synthesis, Characterization and Optical Properties of Low Nuclearity Liganded Silver Clusters: $Ag_{31}(SG)_{19}$ and $Ag_{15}(SG)_{11}$. *Nanoscale* **2013**, *5*, 5637-5643.
15. Bootharaju, M. S.; Pradeep, T. Facile and Rapid Synthesis of a Dithiol-Protected Ag_7 Quantum Cluster for Selective Adsorption of Cationic Dyes. *Langmuir* **2013**, *29*, 8125-8132.
16. Chakraborty, I.; Govindarajan, A.; Erusappan, J.; Ghosh, A.; Pradeep, T.; Yoon, B.; Whetten, R. L.; Landman, U. The Superstable 25 Kda Monolayer Protected Silver Nanoparticle: Measurements and Interpretation as an Icosahedral $Ag_{152}(SCH_2CH_2Ph)_{60}$ Cluster. *Nano Lett.* **2012**, *12*, 5861-5866.
17. Desireddy, A.; Desireddy, Anil C.; Brian E.; Guo, J.;

Yoon, B.; Barnett, R. N.; Monahan, B. M.; Kirschbaum, K.; Griffith, W. P.; Whetten, R. L.; et al. Ultrastable Silver Nanoparticles. *Nature* **2013**, *501*, 399-402.
18. Yang, H.; Wang, Y.; Huang, H.; Gell, L.; Lehtovaara, L.; Malola, S.; Häkkinen, H.; Zheng, N. All-Thiol-Stabilized Ag_{44} and $Au_{12}Ag_{32}$ Nanoparticles with Single-Crystal Structures. *Nat. Commun.* **2013**, *4*.
19. Rao, T. U. B.; Nataraju, B.; Pradeep, T. Ag_9 Quantum Cluster through a Solid-State Route. *J. Am. Chem. Soc.* **2010**, *132*, 16304-16307.
20. Harkness, K. M.; Tang, Y.; Dass, A.; Pan, J.; Kothalawala, N.; Reddy, V. J.; Cliffel, D. E.;Demeler, B.; Stellacci, F.; Bakr, O. M.; et. al. $Ag_{44}(SR)_{30}^{4-}$: A Silver-Thiolate Superatom Complex. *Nanoscale* **2012**, *4*, 4269-4274.
21. Liu, G.; Feng, D.-Q.; Zheng, W.; Chen, T.; Li, D. An Anti-Galvanic Replacement Reaction of DNA Templated Silver Nanoclusters Monitored by the Light-Scattering Technique. *Chem. Commun.* **2013**, *49*, 7941-7943.
22. Diez, I.; Ras, R. H. A. Fluorescent Silver Nanoclusters. *Nanoscale* **2011**, *3*, 1963-1970.
23. Chakraborty, I.; Udayabhaskararao, T.; Pradeep, T. High Temperature Nucleation and Growth of Glutathione Protected Ag_{75} Clusters. *Chem. Commun.* **2012**, *48*, 6788-6790.
24. Liu, S.; Lu, F.; Zhu, J.-J. Highly Fluorescent Ag Nanoclusters: Microwave-Assisted Green Synthesis and Cr^{3+} Sensing. *Chem. Commun.* **2011**, *47*, 2661-2663.
25. Negishi, Y.; Arai, R.; Niihori, Y.; Tsukuda, T. Isolation and Structural Characterization of Magic Silver Clusters Protected by 4-(Tert-Butyl)Benzyl Mercaptan. *Chem. Commun.* **2011**, *47*, 5693-5695.
26. Chakraborty, I.; Udayabhaskararao, T.; Pradeep, T. Luminescent Sub-Nanometer Clusters for Metal Ion Sensing: A New Direction in Nanosensors. *J. Hazard. Mater.* **2012**, *211–212*, 396-403.
27. Guo, J.; Kumar, S.; Bolan, M.; Desireddy, A.; Bigioni, T. P.; Griffith, W. P. Mass Spectrometric Identification of Silver Nanoparticles: The Case of $Ag_{32}(SG)_{19}$. *Anal. Chem.* **2012**, *84*, 5304-5308.
28. Udayabhaskararao, T.; Pradeep, T. New Protocols for the Synthesis of Stable Ag and Au Nanocluster Molecules. *J. Phys. Chem. Lett.* **2013**, *4*, 1553-1564.
29. Zhou, T.; Rong, M.; Cai, Z.; Yang, C. J.; Chen, X. Sonochemical Synthesis of Highly Fluorescent Glutathione-Stabilized Ag Nanoclusters and S^{2-} Sensing. *Nanoscale* **2012**, *4*, 4103-4106.
30. Chakraborty, I.; Udayabhaskararao, T.; Deepesh, G. K.; Pradeep, T. Sunlight Mediated Synthesis and Antibacterial Properties of Monolayer Protected Silver Clusters. *J. Mater. Chem. B* **2013**, *1*, 4059-4064.
31. Mathew, A.; Natarajan, G.; Lehtovaara, L.; Hakkinen, H.; Kumar, R. M.; Subramanian, V.; Jaleel, A.; Pradeep, T. Supramolecular Functionalization and Concomitant Enhancement in Properties of Au_{25} Clusters. *ACS Nano* **2014**, *8*, 139-152.
32. Zheng, K.; Yuan, X.; Kuah, K.; Luo, Z.; Yao, Q.; Zhang, Q.; Xie, J. Boiling Water Synthesis of Ultrastable Thiolated Silver Nanoclusters with Aggregation-Induced Emission. *Chem. Commun.* **2015**, *51*, 15165-15168.
33. Zheng, K.; Setyawati, M. I.; Lim, T.-P.; Leong, D. T.; Xie, J. Antimicrobial Cluster Bombs: Silver Nanoclusters Packed with Daptomycin. *ACS Nano* **2016**, *10*, 7934-7942.
34. Yuan, X.; Setyawati, M. I.; Tan, A. S.; Ong, C. N.; Leong, D. T.; Xie, J. Highly Luminescent Silver Nanoclusters with Tunable Emissions: Cyclic Reduction-Decomposition Synthesis and Antimicrobial Properties. *NPG Asia Mater* **2013**, *5*, e39.
35. Negishi, Y.; Nobusada, K.; Tsukuda, T. Glutathione-Protected Gold Clusters Revisited: Bridging the Gap Between Gold(I)−Thiolate Complexes and Thiolate-Protected Gold Nanocrystals. *J. Am. Chem. Soc.* **2005**, *127*, 5261-5270.
36. Luo, Z.; Zheng, K.; Xie, J. Engineering Ultrasmall Water-Soluble Gold and Silver Nanoclusters for Biomedical Applications. *Chem. Commun.* **2014**, *50*, 5143-5155.
37. Toshima, N.; Kanemaru, M.; Shiraishi, Y.; Koga, Y. Spontaneous Formation of Core/Shell Bimetallic Nanoparticles: A Calorimetric Study. *J. Phys. Chem. B* **2005**, *109*, 16326-16331.
38. Pierce, M. M.; Raman, C. S.; Nall, B. T. Isothermal Titration Calorimetry of Protein–Protein Interactions. *Methods* **1999**, *19*, 213-221.
39. Rajarathnam, K.; Rösgen, J. Isothermal Titration Calorimetry of Membrane Proteins — Progress and Challenges. *Biochimica et Biophysica Acta (BBA) - Biomembranes* **2014**, *1838*, 69-77.
40. Chakraborty, I.; Pradeep, T. Reversible Formation of Ag_{44} from Selenolates. *Nanoscale* **2014**, *6*, 14190-14194.
41. Ravi, V.; Binz, J. M.; Rioux, R. M. Thermodynamic Profiles at the Solvated Inorganic-Organic Interface: The Case of Gold-Thiolate Monolayers. *Nano Lett.* **2013**, *13*, 4442-4448.
42. Freyer, M. W.; Lewis, E. A. Isothermal Titration Calorimetry: Experimental Design, Data Analysis, and Probing Macromolecule/Ligand Binding and Kinetic Interactions. *Methods Cell Biol.* **2008**, *84*, 79-113.
43. Bootharaju, M. S.; Pradeep, T. Investigation into the Reactivity of Unsupported and Supported Ag_7 and Ag_8 Clusters with Toxic Metal Ions. *Langmuir* **2011**, *27*, 8134-8143.
44. Bellina, B.; Compagnon, I.; Bertorelle, F.; Broyer, M.; Antoine, R.; Dugourd, P.; Gell, L.; Kulesza, A.; Mitrić, R.; Bonačić-Koutecký, V. Structural and Optical Properties of Isolated Noble Metal–Glutathione Complexes: Insight into the Chemistry of Liganded Nanoclusters. *J. Phys. Chem. C* **2011**, *115*, 24549-24554.
45. Shen, J.-S.; Li, D.-H.; Zhang, M.-B.; Zhou, J.; Zhang, H.; Jiang, Y.-B. Metal−Metal-Interaction-Facilitated Coordination Polymer as a Sensing Ensemble: A Case Study for Cysteine Sensing. *Langmuir* **2011**, *27*, 481-486.
46. Dreier, T. A.; Ackerson, C. J. Radicals Are Required for Thiol Etching of Gold Particles. *Angew. Chem., Int. Ed.* **2015**, *54*, 9249-9252.

TOC Graphic

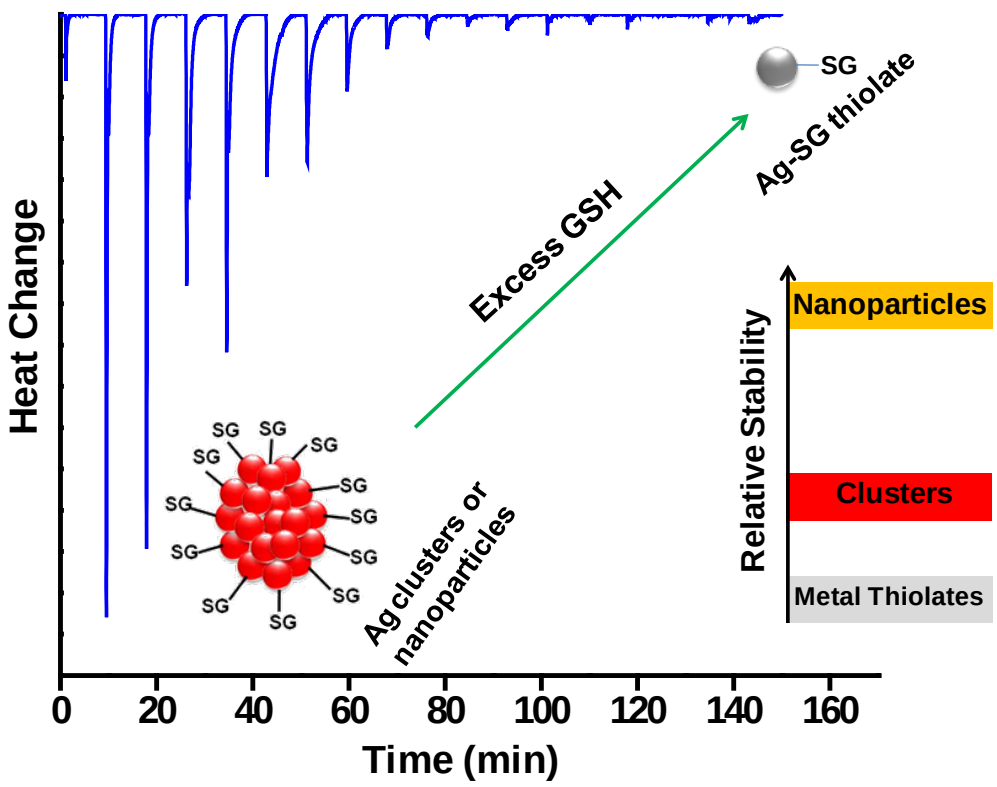
Heat Change
Time (min)
0
20
40
60
80
100
120
140
160
Excess GSH
SG
Ag-SG thiolate
Ag clusters or nanoparticles
Relative Stability
Nanoparticles
Clusters
Metal Thiolates